# Statistical evaluation of backscattered ultrasonic grain signals

Jafar Saniie and Tao Wang
*Department of Electrical and Computer Engineering, Illinois Institute of Technology, Chicago, Illinois 60616*

Nihat M. Bilgutay
*Department of Electrical and Computer Engineering, Drexel University, Philadelphia, Pennsylvania 19104*

(Received 20 December 1987; accepted for publication 27 March 1988)

Insonification of the microstructure of materials results in a backscattered signal consisting of multiple interfering echoes with random amplitudes and phases. Information pertaining to grain scattering cross section and grain size distribution is an inherent property of the backscattered signal. A statistical model of grain signals is developed that describes the spatial and time averaged data, and their relationship to signal attenuation caused by scattering and absorption. Both spatial and temporal averaging permits the estimation of the attenuation coefficient, which has been found to be position dependent. Furthermore, it has been shown experimentally and theoretically that the performance of spatial and time averaging is governed by correlation properties of the grain signal.

PACS numbers: 43.20.Fn, 43.35.Cg, 43.35.Zc

## INTRODUCTION

The importance of grain size estimation has long been recognized in examining many inherent mechanical properties such as strength and toughness,[1,2] and the magnetic properties of some materials.[3,4] Among the various methods for evaluating the microstructure of materials, the utilization of the ultrasonic backscattered signal has been proven to be a simple and efficient method of nondestructive testing. Most studies dealing with ultrasonic microstructure evaluation are based on comparison of the attenuation coefficient of specimens with unknown grain sizes to specimens with known grain sizes under similar experimental conditions. The attenuation measurement is generally accomplished either by comparing the front and back surface echoes of a specimen of known thickness using the pulse-echo mode, or by comparing the intensity of the pulse through the unknown specimen with that of the calibrated specimen using the transmission mode. Both methods have some practical limitations[5]: (a) Flat and parallel surfaces are important for efficient measurement; (b) since the measured attenuation coefficient represents an average value over the entire propagation path, the local variations of the attenuation coefficient cannot be obtained; and (c) good coupling between the transducer and sample is essential for minimum energy losses.

The backscattered grain echoes are random signals that bear information related to the attenuation properties of the materials. The variation of attenuation as a function of position represents statistical changes in the scattering cross section and absorption properties of grains. It must be noted that attenuation in the backscattered field is influenced by many random physical parameters such as grain size, grain shape (elongated, flattened, equiaxed, or mixture), grain orientation (random or preferred), quality of grain boundaries (presence or absence of voids or inclusions), and the proportion of chemical constituents.[6] Some earlier research efforts have been directed at characterizing the statistical relationships between the energy of the ultrasonic propagation wave and the local variation of the scatterers. Beecham[7] was able to demonstrate that the attenuation of backscattered echoes with depth is related to the average grain size of the specimen. Aldridge[8] confirmed Beecham's results and concluded that the distribution of grain scattering cross section can be obtained through multiple measurements of nonoverlapping scattering regions. Fay[9] and Goebbels *et. al.*[5,10,11] further improved this idea to more accurately determine the expected amplitude of the backscattered echoes with respect to depth by utilizing various averaging techniques, namely spatial, directional, and frequency averaging. Saniie and Bilgutay[12] demonstrated various grain size characterization techniques that extract parameters from the backscattered signal related to the frequency-dependent attenuation coefficient.

In this article, we present a statistical comparison of the time averaging method accomplished using a single $A$-scan and ensemble averaging that requires multiple measurements obtained by changing the position of the transducer. The backscattered grain signal is represented by a mathematical model and is used for obtaining the ultrasonic attenuation coefficient. Correlation effects on the performance of attenuation estimation and the local variation of attenuation coefficients are discussed. Finally, both ensemble and time averaging are implemented for characterizing the grain size in steel samples. Recommendations are provided based on the comparison of experimental results and theoretical predictions.

## I. GRAIN ATTENUATION

When an ultrasonic burst of sound travels through an inhomogeneous materials, its amplitude is attenuated as

$$A_z = A_0 e^{-\int_0^z \alpha(z,f)\,dz}, \tag{1}$$

where $A_0$ is the initial amplitude, $A_z$ is the amplitude at the given position $z$ corresponding to time $t$, and $\alpha(z,f)$ is the

 0001-4966/88/070400-09$00.80  

TABLE I. Scattering coefficients as function of grain diameter and frequency.

| Scattering region | Scattering function | Relationships |
|---|---|---|
| Rayleigh | $C_1 D^3 f^4$ | $\lambda \gg D$ |
| Stochastic | $C_2 D f^2$ | $\lambda \simeq D$ |
| Diffusive | $C_3/D$ | $\lambda \ll D$ |

position and frequency-dependent attenuation coefficient. If materials exhibit homogeneous properties as a function of position $z$, the above equation can be simplified to

$$A_z = A_0 e^{-\alpha(f)z}, \tag{2}$$

where $\alpha(z,f) = \alpha(f)$. In general, the attenuation coefficient has two major causes:

$$\alpha(f) = \alpha_a(f) + \alpha_s(f), \tag{3}$$

where the term $\alpha_a(f)$ is a hysteresis loss caused mainly by the inelastic behavior of the materials, and the term $\alpha_s(f)$ is a scattering loss mainly associated with the characteristics of grain and phase boundaries (acoustical impedance discontinuities). In many practical situations, grain scattering loss at ultrasonic frequencies is so large relative to the hysteresis loss that the latter is negligible. The scattering formulas have been studied and classified into distinct scattering regions according to the ratio of the sound wavelength $\lambda$ to the mean grain diameter $\bar{D}$ (Refs. 13–15). The functions are tabulated in Table I.

In this study, experiments were conducted in the Rayleigh scattering region. Details concerning the scattering constants (i.e., the constants $c_1$, $c_2$, $c_3$ as shown in Table I) for both cubic and hexagonal grains can be found in the articles by Papadakis.[16,17] Of the three scattering regions, the Rayleigh scattering ($\lambda \gg \bar{D}$) exhibits the most sensitivity to the frequency and grain size distribution. In addition, the multiple scattering is considered to be negligible, which simplifies the localization of scatterers and their scattering properties.

## II. A STATISTICAL MODEL OF GRAIN SIGNAL

The measured grain backscattered echo is a composite signal corresponding to many reflected grain boundary echoes with random amplitudes and arrival times. As shown in Fig. 1, in a given range cell, the random scatterers can be represented by delta functions, and the grain characteristic function can be represented by the sum of these delta functions:

$$g(t) = \sum_{k=1}^{M} A_k \delta(t - \tau_k), \tag{4}$$

where the range cell at the position corresponding to the round-trip time $t$ represents a small time interval of size $2\epsilon$:

$$t - \epsilon < \tau_k < t + \epsilon, \quad \forall k. \tag{5}$$

Note that $M$ is a random variable and represents the total number of scatterers within the range cell. The term $A_k$ is defined as

$$A_k = \sigma_{sk} e^{-\alpha \tau_k}, \tag{6}$$

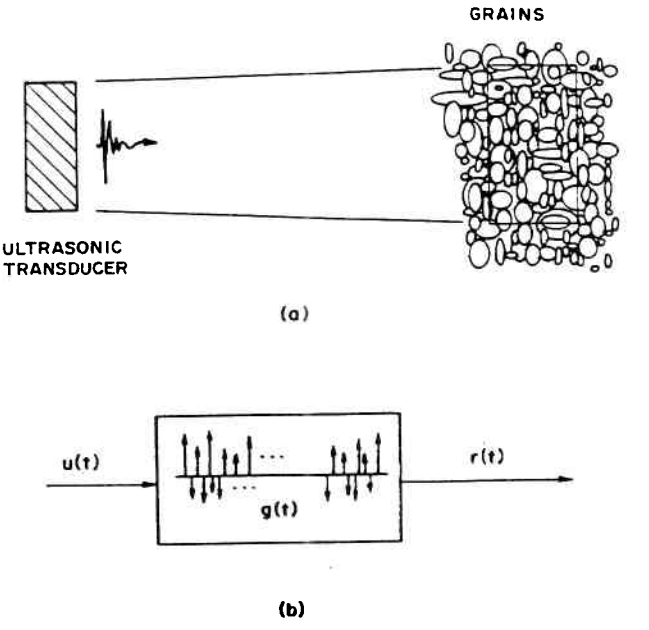


FIG. 1. (a) Range cell geometry; (b) grain scattering model.

where $\sigma_{sk}$ is a random variable related to the grain scattering cross section, and $e^{-\alpha \tau_k}$ is the result of attenuation that depends on the position of the scatterers within the range cell. It is important to point out that, although both the scattering coefficient $\sigma_{sk}$ and the attenuation coefficient $\alpha$ are functions of frequency, this is omitted in the above equation in order to simplify the mathematical representation.

Based on the properties of linear system theory, the measured signal is

$$r(t) = u(t) * g(t) = \sum_{k=1}^{M} A_k u(t - \tau_k), \tag{7}$$

where $u(t)$ is the basic ultrasonic wavelet, as shown in Fig. 2. Without loss of generality, we make the assumption that the wavelet has Gaussian envelope,

$$u(t) = e^{-\gamma t^2} e^{j\omega t}, \tag{8}$$

where $\omega$ is the center frequency and $\gamma$ is a constant representing the reciprocal square of the width of the wavelet in time.

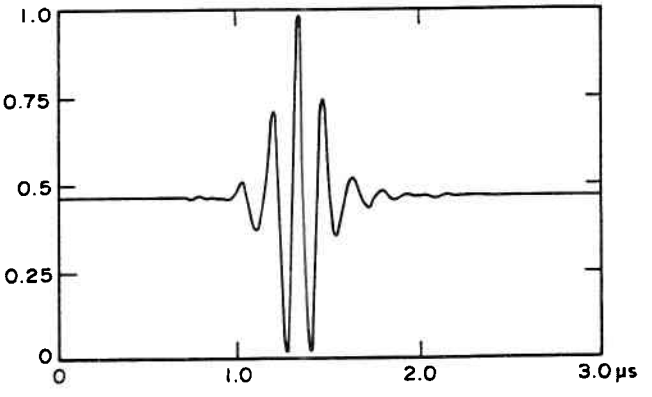


FIG. 2. A typical ultrasonic wavelet.

Using Eq. (8), the grain signal corresponding to range cell centered about roundtrip time $t$ becomes

$$r(t) = \sum_{k=1}^{k} \sigma_{sk} e^{-\alpha\tau_k} e^{j\omega(t-\tau_k)} e^{-\gamma(t-\tau_k)^2}. \quad (9)$$

For $\epsilon$ on the order of a period and $t \gg \epsilon$ (farfield region), $e^{-\alpha\tau_k} \approx e^{-\alpha t}$ and Eq. (9) will simplify to

$$r(t) = e^{-\alpha t} \sum_{k=1}^{M} \sigma_{sk} e^{j\phi k}, \quad \phi_k = (t-\tau_k)\omega. \quad (10)$$

Note that the random phase $\phi_k$ is governed by the random arrival time of echoes and is considered to be uniformly distributed from 0 to $2\pi$. Let us define

$$Re^{j\theta} = \sum_{k=1}^{M} \sigma_{sk} e^{j\phi_k}. \quad (11)$$

Then,

$$r(t) = Re^{j\theta} e^{-\alpha t}. \quad (12)$$

As shown in Fig. 3, the term $Re^{j\theta}$ given in Eq. (11) can be resolved into $X$ and $Y$ components[18]:

$$X = \sum_{k=1}^{M} X_k = \sum_{k=1}^{M} \sigma_{sk} \cos\phi_k, \quad (13)$$

$$Y = \sum_{k=1}^{M} Y_k = \sum_{k=1}^{M} \sigma_{sk} \sin\phi_k. \quad (14)$$

In practice, the number of scatterers illuminated by the transducer is very large, and the scatterers are considered to be independent and identically distributed (i.i.d). Therefore, according to central limit theorem, for large $M$, $X$ and $Y$ are normally distributed. The mean of random variable $X$ and $Y$ is

$$E(X) = E\left[E\left(\sum_{k=1}^{M} \sigma_{sk} \cos\phi_k\right)\right], \quad (15)$$

$$E(Y) = E\left[E\left(\sum_{k=1}^{M} \sigma_{sk} \sin\phi_k\right)\right]. \quad (16)$$

Since the random variables $M$, $\sigma_{sk}$ and $\phi_k$ are considered to be independent, and $\phi_k$ is uniformly distributed over the range $(0,2\pi)$, the expected value of the random variables $X$ and $Y$ is zero. The variance of $X$ and $Y$ are[18]:

$$\sigma_X^2 = \sigma_Y^2 = \tfrac{1}{2}E(M)E(\sigma_{sk}^2) = \sigma^2. \quad (17)$$

Furthermore, it can be proven that $X$ and $Y$ are uncorrelated:

$$E(XY) = E(X)E(Y) = 0. \quad (18)$$

Using Eqs. (15)–(18), the joint probability density of $X$ and $Y$ is obtained:

$$f_{XY}(x,y) = f_X(x) f_Y(y) = (1/2\pi\sigma^2) e^{-(x^2+y^2/2\sigma^2)}. \quad (19)$$

The distribution of the amplitude of the backscattered grain signal, $f_R(r)$, can be achieved by using the following relations[19]:

$$X = R\cos\theta, \quad (20)$$

$$Y = R\sin\theta, \quad (21)$$

$$f_R(r) = \int_0^{2\pi} f_{R\theta}(r,\theta)\, d\theta, \quad (22)$$

and that is

$$f_R(r) = (2r/\eta) e^{-r^2/\eta}, \quad (23)$$

where

$$\eta = E(M)E(\sigma_s^2). \quad (24)$$

Equation (23) is referred to as the Rayleigh probability density function, whose validity has been confirmed experimentally based on the amplitude histograms of grain signals from steel samples (type 1018) of different grain sizes. Prior to constructing the histograms, the grain signals were filtered by an envelope detector and normalized by removing the effect of attenuation. Figure 4 shows the histograms of the grain signals backscattered from two different steel samples with grain sizes of 14 and 50 $\mu$m. As shown in this figure, the histograms (solid line) fit the Rayleigh probability den-

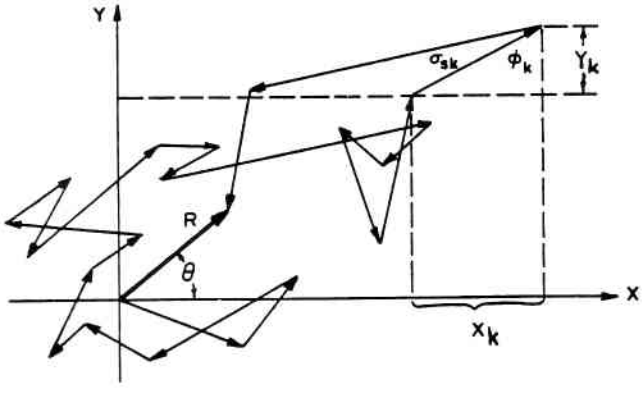


FIG. 3. A random phasor sum in the complex plane.[25]

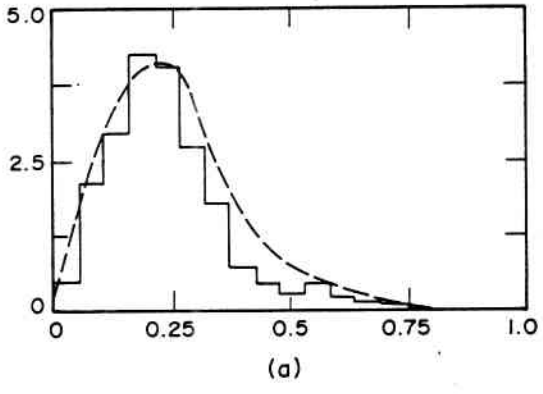


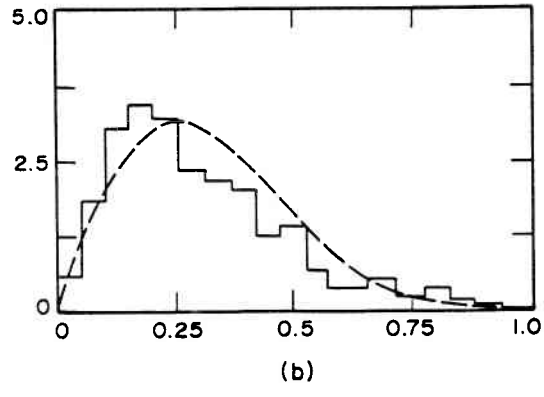


FIG. 4. Amplitude histograms of grain signals: (a) steel, (b) steel-2000.

sity function (dash line) very closely. These results are representative of numerous experimental observations. It should be noted that, although our experimental results show a close fit to Rayleigh distribution, in practice, this may not always be the case for all materials. A similar study has been carried out in radar to evaluate clutter,[20,21] and a broad range of probability density functions has been reported.

## III. ESTIMATION OF ATTENUATION

One of the objectives of evaluating the backscattered signal is to extract the attenuation coefficient. Equation (12) indicates that the measured signal $r(t)$ has a random pattern, and attenuation can only be obtained by performing some sort of averaging. Using Eqs. (23) and (24), the expected value of the amplitude of the backscattered signal results in

$$E[r(t)] = (e^{-\alpha t}/2)\sqrt{E(M)E(\sigma_s^2)\pi} = C_1 e^{-\alpha t}. \quad (25)$$

Inspection of Eq. (25) reveals that the expected grain signal is attenuated exponentially as a function of time, and the intensity is proportional to the grain scattering cross section. Based on the above equations, the attenuation coefficient can be obtained from the ensemble average of the grain signals at a given time. In general, a better estimate of the attenuation coefficient can be obtained by estimating $E[r(t)]$ using ensemble averages at many different times and applying linear regression after logarithmic transformation. The overall system of estimating the attenuation coefficient is shown in Fig. 5. The key to the accuracy of the measurement is the effectiveness of the averaging operation. In the following sections, we present the mathematical analysis of two averaging techniques—spatial and temporal—for obtaining the expected value of the grain signal.

### A. Spatial averaging

Spatial averaging is a method for characterizing attenuation as a function of position. This can be accomplished by scanning the specimen and averaging the rectified backscattered signals. Let us assume that averaging of $N$ measurements at $N$ different positions of the specimen is performed:

$$\langle r(t)\rangle = \frac{1}{N}\sum_{i=1}^{N} \hat{r}_i e^{-\alpha t}, \quad (26)$$

where $\hat{r}_i e^{-\alpha t}$ is the rectified backscattered signal measured at a given position $i$. In general, for homogeneous materials, the signal amplitude is wide-sense stationary that implies

$$E(\hat{r}_i) = m \quad (27)$$

$$E(\hat{r}_i \hat{r}_j) = R_s(k), \quad \forall k = |i-j|. \quad (28)$$

Except for the scaling factor $m$, Eq. (26) is an unbiased estimator of attenuation:

$$E[\langle r(t)\rangle] = me^{-\alpha t}. \quad (29)$$

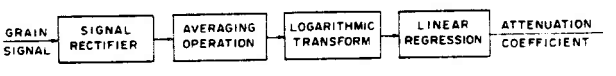


FIG. 5. System block diagram for attenuation measurements.

Furthermore, using Eqs. (27)–(29), the variance of $\langle r(t)\rangle$ can be determined:

$$\sigma^2_{\langle r(t)\rangle} = e^{-2\alpha t}(\sigma_r^2/N) + e^{-2\alpha t}\frac{1}{N^2}\sum_{k=1}^{N-1}\{2(N-k)[R_s(k)-m^2]\}. \quad (30)$$

If the spacing between measurements is large, the ensemble measurements will be uncorrelated. Hence,

$$R_s(k) = m^2, \quad k \neq 0 \quad (31)$$

and

$$\sigma^2_{\langle r(t)\rangle} = e^{-2\alpha t}(\sigma_r^2/N). \quad (32)$$

In the above equation, as $(N \to \infty)$, the term $\sigma^2_{\langle r(t)\rangle} \to 0$. This is the condition for obtaining a consistent estimate of $\langle r(t)\rangle$. In practice, the ensemble measurements are not necessarily uncorrelated $[R_s(k) \neq m^2]$ and, consequently, the effective number of independent averagings is expected to be less than the actual value of $N$.

### B. Time averaging

Another practical approach to ensemble averaging is time domain averaging. The grain signal is a stochastic process in which randomness is inherent to any single measurement. The temporal fluctuations contain equivalent information to the random spatial fluctuations; therefore, it is appropriate to determine the statistical parameters (e.g., mean and variance) of the process from a single measurement, which is far more practical than using multiple measurements. This approach is valid when using stationary random processes in which time averages are identical to their ensemble averages (i.e., ergodic process[22]).

Time averaging is accomplished by averaging samples of the rectified grain signal taken at time $t + \Delta t, \ldots, t + N\Delta t$, such that

$$\overline{r(t)} = \frac{1}{N}\sum_{i=1}^{N} \hat{r}_i e^{-\alpha(t+i\Delta t)}, \quad (33)$$

where $\hat{r}_i$ is the amplitude of unattenuated signal corresponding to given time $t + i\Delta t$. In the above equation, the sum represents averaging of $N$ random variables weighted by $e^{-\alpha i\Delta t}$. The $\hat{r}_i$ is a stationary random process, and the expected value of Eq. (33) becomes

$$E[\overline{r(t)}] = \frac{e^{-\alpha t}}{N} m \sum_{i=1}^{N} e^{-\alpha i\Delta t}, \quad (34)$$

where $m = E(\hat{r}_i)$. Let us assume the integration period $T$ is equal to $N\Delta t$, and the term $T$ remains constant as $N \to \infty$. Then, Eq. (34) is simplified to

$$E[\overline{r(t)}] = e^{-\alpha t}\{E(\hat{r})[(1-e^{-\alpha T})/\alpha T]\}. \quad (35)$$

Once $T$ is defined, the term $(1-e^{-\alpha T})/\alpha T$ becomes a known constant. Similar to spatial averaging, time domain integration of the amplitude signal is equal to the attenuation factor $e^{-\alpha t}$, multiplied by a constant [Eq. (35)]. Therefore, time averaging [Eq. (33)] is an unbiased estimator of the attenuation. The accuracy of the estimation is highly dependent on the value of $\sigma^2_{\overline{r(t)}}$.

Let us define the temporal autocorrelation of the sampled signal as

$$R_t(|i-j|) = E(\hat{r}_i \hat{r}_j), \tag{36}$$

then, the second moment of $\overline{r(t)}$ can be represented in terms of the autocorrelation functions:

$$E[\overline{r(t)}^2] = \frac{e^{-2\alpha t}}{N^2}\left(R_t(0)\sum_{i=1}^{N} e^{-2\alpha i\Delta t} + \sum_{i=1}^{N}\sum_{j=1,i\neq j}^{N} e^{-\alpha(i+j)\Delta t} R_t(|i-j|)\right). \tag{37}$$

Using Eqs. (34) and (37), the variance of $\overline{r(t)}$ can be obtained:

$$\sigma^2_{\overline{r(t)}} = \frac{e^{-2\alpha t}}{N^2}\left(\sigma^2_{\hat{r}}\sum_{i=1}^{N} e^{-2\alpha i\Delta t} + \sum_{i=1}^{N}\sum_{j=1,i\neq j}^{N} e^{-\alpha(i+j)\Delta t}[R_t(|i-j|) - m^2]\right), \tag{38}$$

where $\sigma^2_{\hat{r}}$ is the variance of $\hat{r}_i$. Let us define,

$$\sigma^2_{co}(k) = R_t(|i-j|) - m^2. \tag{39}$$

Hence, the variance can be rewritten as

$$\sigma^2_{\overline{r(t)}} = \frac{e^{-2\alpha t}}{N^2}\left(\sigma^2_{\hat{r}}\frac{1-e^{-2\alpha T}}{2\alpha\Delta t} + \frac{2e^{-2\alpha\Delta t}}{1-e^{-2\alpha\Delta t}}\sum_{k=1}^{N-1}\sigma^2_{co}(k) \times (e^{-\alpha k\Delta t} - e^{-2\alpha N\Delta t + k\Delta t\alpha})\right). \tag{40}$$

If the sample values are uncorrelated, the term $\sigma^2_{co}(k)$ becomes zero for all $k$. Under this condition, the variance of the estimation simplifies to

$$\sigma^2_{\overline{r(t)}} = (\sigma^2_{\hat{r}}/N)[e^{-2\alpha t}(1-e^{-2\alpha T})/2\alpha T]. \tag{41}$$

If $N\rightarrow\infty$, and $\sigma^2_{\overline{r(t)}}\rightarrow 0$, then the estimation becomes consistent. It is important to point out that, for a small value of $\alpha T$, the mean and variance associated with temporal averaging become identical to spatial averaging. This equality is only true with conditions of ergodicity, stationarity, and when using uncorrelated observations. As with spatial averaging, the effective number of time averages is less than the actual value of $N$ when the sampled values of the signal are correlated. Furthermore, the accuracy or reliability of time averaging is highly dependent on the choice of $T$. From an analytical point of view, the larger the value of $T$, the better the estimate can be. But when $T$ is assigned a large value, signal attenuation becomes significant, causing poor signal-to-noise ratio that will introduce error in the estimation.

## IV. TEMPORAL AND SPATIAL AVERAGING RESULTS

The object of this work is to evaluate the grain size variation in solids when other physical parameters (e.g., crystal shape, elastic constants, density, and velocities) remain constant. These assumptions allow us to accurately interpret the measurements resulting from the grain size variation. In this study, type 1018 steel blocks ($4\times4\times10$ in.) were heat treated for 4 h to obtain various grain sizes. Microstructures of the samples are shown in Fig. 6. Type 1018 steel sample has an average grain size of 14 $\mu$m prior to heat treatment and the grain size increases to 24 and 50 $\mu$m with heat treatment at 1700 and 2000 °F, respectively.

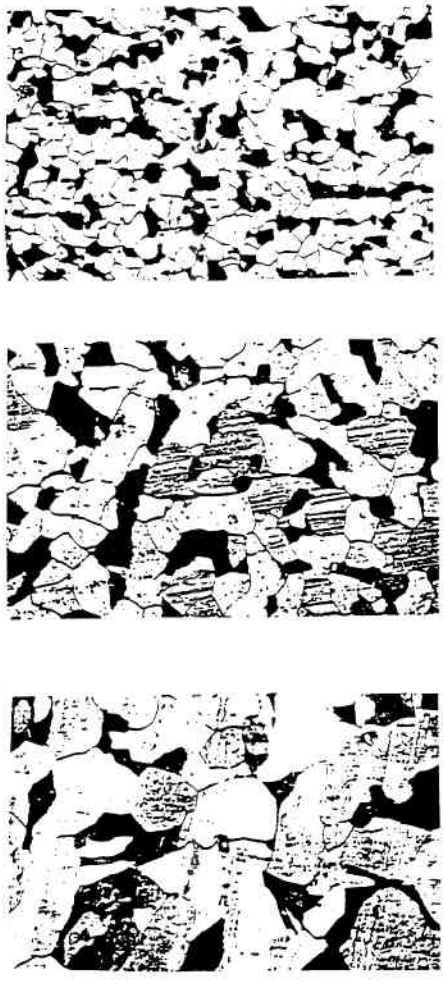


FIG. 6. Micrographic results of steel samples: (a) no heat treatment, (b) heat treatment at 1700 °F, (c) heat treatment at 2000 °F.

The experimental grain signal measurements were accomplished using a Gamma type transducer manufactured by K-B Aerotech with approximately a 5-MHz center frequency and 3-dB bandwidth of approximately 1.5 MHz. The rf signal was sampled at 100 MHz with 8-bits resolution. All measurements were carried out using an immersion technique with the specimens being placed in the farfields of the transducer. The transducer aperture is 0.5 in. and, therefore, significant spacing between measurements is required for obtaining uncorrelated data. The scanning area is square shaped covered by a $16\times16$ grid. Figure 7 shows spatial averaging results corresponding to various scanning areas: $0.5\times0.5$, $0.75\times0.75$, $1.0\times1.0$, and $2.0\times2.0$ in. All measurements clearly display the effect of attenuation in the signal. It should be noted that there is more variation in the rate of decay in data corresponding to smaller scan areas (e.g., $0.5\times0.5$ in.) than the larger areas (e.g., $2.0\times2.0$ in.). This is due to the higher degree of correlation between measurements when using a small area of scanning. For different grain size samples, the attenuation coefficient was estimated using the procedure described earlier in Fig. 5. The grain

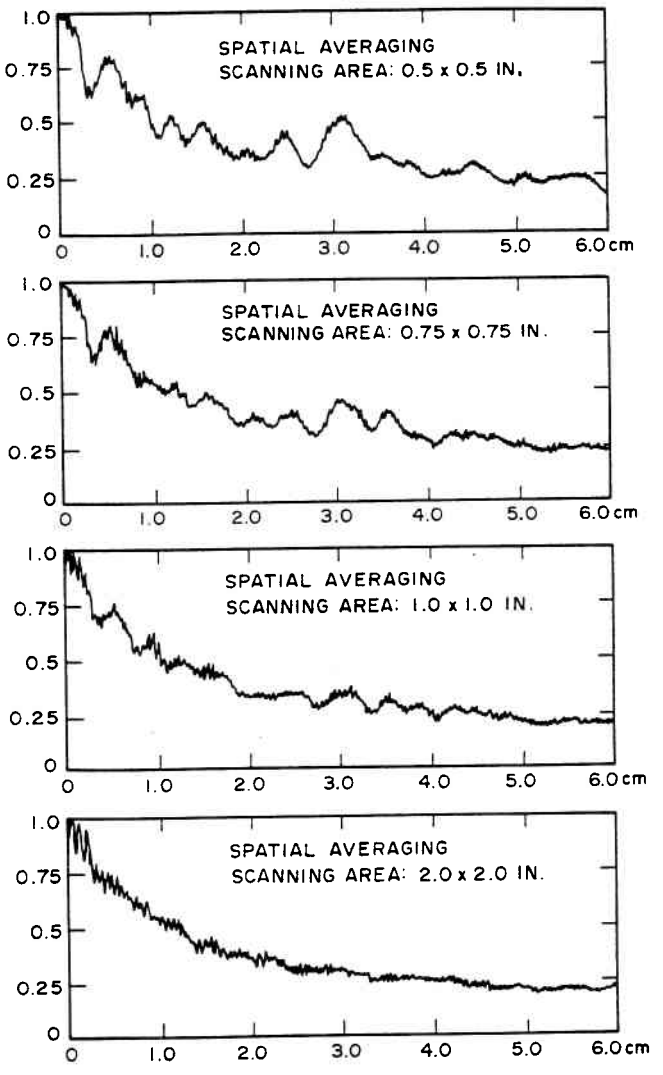


FIG. 7. Comparison of the backscattered grain signals using different scanning area for spatial averaging.

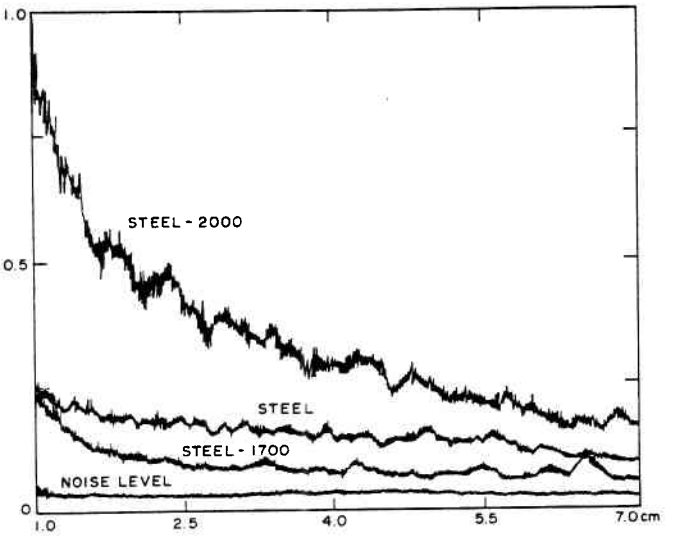


FIG. 8. Spatial averaging of backscattered ultrasonic signals from steel samples with different grain sizes.

signal used for estimating the attenuation coefficient represents scattering characteristics in the region between 0.40 and 2.75 in. from the front surface of the specimen. Consistent estimates of attenuation coefficients (i.e., $\pm 5\%$ variation) are obtained within a 2.0-$\times$2.0-in. scanning area.

A comparison of ensemble averaging results corresponding to samples of various grain sizes is shown in Fig. 8. The four measurements shown in this figure were obtained under identical experimental conditions (i.e., the position of transducer with respect to samples, the angle of incident beam, and the pulser, receiver, and digitizer adjustments) using ensemble averaging of a 2-$\times$2-in. scanning area of specimen covered by $16\times16$ grids. The top three traces represent the ensemble averaging of backscattered signal corresponding to different grain sizes. The lower trace is the system noise level in the absence of the grain signal. The duration of the signals are 20 $\mu$s, while the starting points are 3.5 $\mu$s away from the front surface echoes. These signals provide information corresponding to a region between 0.40 to 2.75 in. inside the steel samples. As evident from Fig. 8, the samples with larger grain sizes scatter echoes of larger intensity compared to samples of smaller grain sizes. In general, the intensity of the backscattered signal can be correlated with the grain size, although one must be aware that this intensity is highly dependent on the geometry of the specimen and the beam angle of incidence. Furthermore, all three traces of the grain signals display attenuation effects. The estimates of the attenuation coefficients in the steel samples obtained using spatial averaging are presented in Table II. The attenuation coefficients are estimated by utilizing the entire 2048 data points and applying the steps involved in the model shown in Fig. 5.

Through extensive experimentation and evaluation of the backscattered grain signal, we have observed that the attenuation coefficient is position dependent, which creates ambiguity in the interpretation of the results. An experimental evaluation of this problem is discussed later. Nevertheless, graphical results shown in Fig. 8, and the numerical values presented in Table II, indicate the feasibility and potential of attenuation measurement as a method for nondestructive grain size characterization.

A similar study has been performed using temporal averaging. As discussed in the theoretical section, the number of samples and sampling intervals is essential in obtaining consistent averaging results. To evaluate temporal averaging performance, window lengths between 64 to 512 samples were examined. Experimental results of the time averaging using different window sizes are shown in Fig. 9. It

TABLE II. Estimated attenuation coefficients for different grain sizes.

| Steel | Heat-treated temperature (°F) | Estimated grain size ($\mu$m) | Estimated attenuation coefficient (dB/cm) |
|---|---|---|---|
| Steel | ... | 14 | 0.6226 |
| Steel-1700 | 1700 | 24 | 0.8252 |
| Steel-2000 | 2000 | 50 | 1.139 |

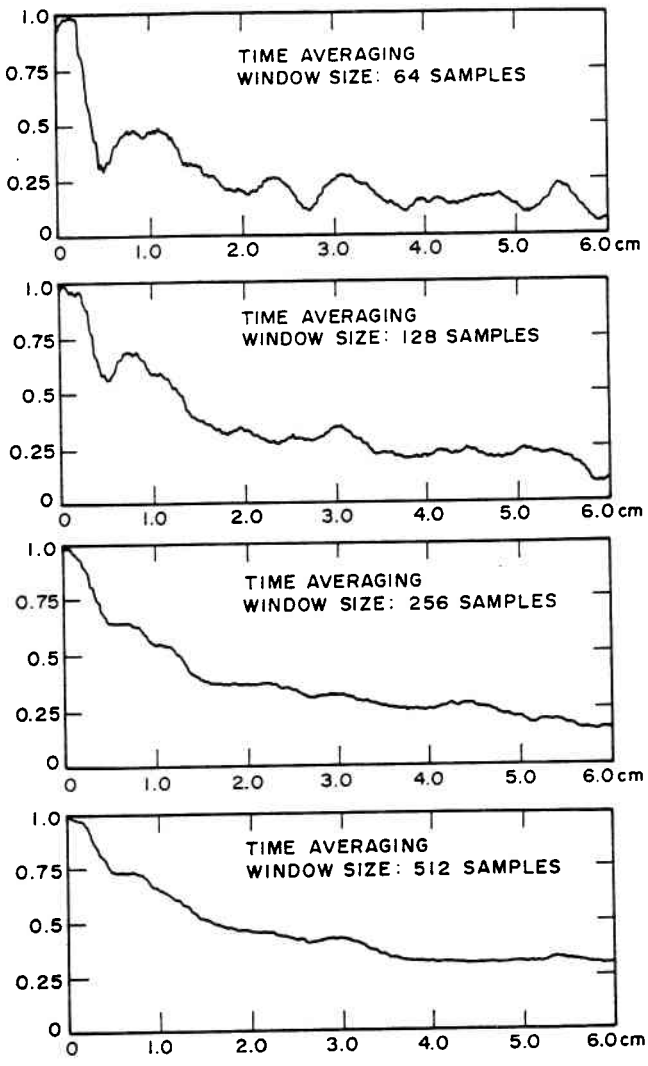


FIG. 9. Temporal averaging of ultrasonic grain signal using different window lengths.

should be noted that with temporal averaging there is significant variation in the rate of decay corresponding to smaller window sizes. Estimating the attenuation coefficient using temporal averaging based on the methods shown in Fig. 5 appears to be consistent to within $\pm$ 10%. These observations suggest that temporal averaging is a good substitute for spatial averaging. For the steel specimens examined, results of spatial and temporal averaging have been very similar. An example is shown in Fig. 10. In general, using a single $A$ scan is more practical and efficient for ultrasonic testing. In fact, in some situations, the geometry of the object interferes with or prohibits the use of multiple measurements. Furthermore, if the penetration of ultrasonic energy is position or orientation dependent, an assessment of this variation is necessary and must be compensated prior to averaging. Finally, and most importantly, the use of a single measurement reveals information confined to a smaller region of the sample relative to the average of multiple measurements that displays integrated information pertaining to a broader region of the sample.

### A. Correlation effects

As discussed earlier, for both temporal and spatial averaging, correlation among repeated measurements plays an important role in the effectiveness in smoothing process. This fact can be confirmed by the basic principles of information theory.[23] The average mutual information between measurement $X$ and measurement $Y$ is given by

$$I(X;Y) = H(X) - H(X/Y), \tag{42}$$

where $H(X)$ is the average self-information (entropy) of measurement $X$, and $H(X/Y)$ is the conditional information of measurement $X$ when measurement $Y$ has already been carried out. If measurement $X$ is independent of measurement $Y$, then, the average mutual information $I(X;Y) = 0$, and conditional entropy $H(X/Y)$ for measurement $X$ given measurement $Y$ is equal to the information provided by measurement $X$. In order to illustrate the measurement performance in terms of the self-information provided by the individual measurement, we introduce the effective number of independent measurements $N_e$, defined as

$$N_e = \frac{\text{variance at the averager input}}{\text{variance at the averager output}}. \tag{43}$$

If all measurements are independent, $N_e = N$, then the effect of the averager is to reduce the variance of the random averaging signal by a factor of $N$. If all measurements are completely correlated, then $N_e = 1$, and there is no reduction in the variance of the random averaging signal.

The correlation properties and the effective number $N_e$ of the measured signals were examined. The estimated effective number $N_e$ for both temporal and ensemble averaging is

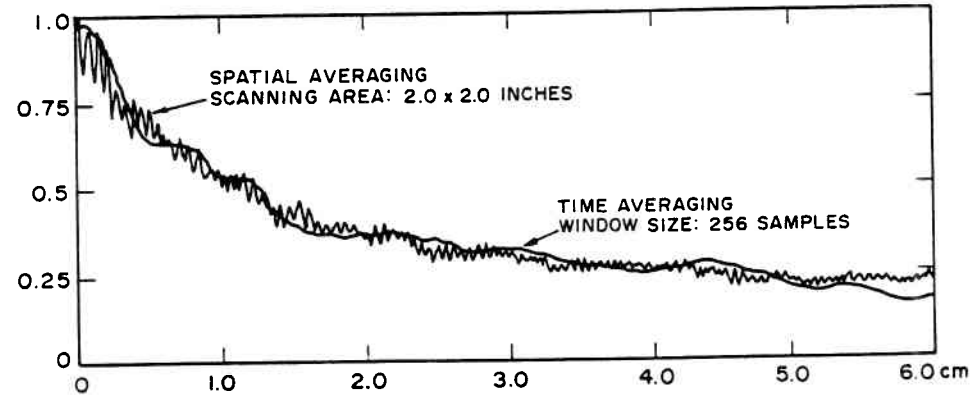


FIG. 10. A comparison of spatial averaging and temporal averaging.

TABLE III. Performance of spatial averaging.

| Scanning area | 0.5×0.5 in. | 0.75×0.75 in. | 1.0×1.0 in. | 2.0×2.0 in. | 2.0×8.0 in. |
|---|---|---|---|---|---|
| Actual $N$ | 256 | 256 | 256 | 256 | 1024 |
| Variance (0.1445) | 0.017 | 0.015 | 0.006 | 0.002 | 0.0003 |
| Effective $N$ | 8.6 | 9.6 | 24.5 | 58.5 | 437.7 |
| Normalized effective $N$ | 3% | 4% | 10% | 22% | 44% |

presented in Tables III and IV. In Table III, the effective number was computed by using Eq. (43), and the results were normalized by the actual number of measurements. We note that the normalized effective number of measurements becomes larger as the scanning area increases. This suggests that there is less correlation among grain signals if they are measured at positions farther apart. Similar conclusions can be reached in measurements involving temporal averaging. Table IV shows the normalized effective number of measurements corresponding to different window lengths. As the integration time increases, the performance of averaging improves and the normalized effective number increases. It must be noted that, since a high correlation exists between the sucessive sample values of the grain signal, the effective number is significantly smaller than the total number of sample values, as shown in Table IV.

An evaluation of the autocorrelation [Eq. (36)] and the ensemble correlation [Eq. (28)] is shown in Fig. 11. This figure supports the principle of ergodicity, since a great degree of similarity exists between the pattern of autocorrelation and ensemble correlation. Furthermore, both autocorrelation and ensemble correlation values are high for a small shift in position (e.g., within 0.1 in.), although beyond 0.2 in. the correlation drops as much as 80%. The correlation for data collected at positions farther apart fluctuates around 20%, which implies that the ratio of $N_e/N$ will not reach the ideal value of unity. Regardless of the low value for $N_e/N$, one can conclude that a spacing larger than 0.1 in. is desirable between sequential measurements. In fact, this condition was satisfied in the spatial averaging of a 2-×2-in. area scanned using a 16×16 grid. For this situation, $N_e/N$ is about 25%, which is far less than unity.

### B. Grain signal attenuation behavior

In the process of estimating the attenuation coefficient, we have observed that attenuation is position dependent. The rate of decay of grain signal is initially large and drops as time proceeds. This suggests that the attenuation characteristics are not a simple exponential decay process at all, although such a model seems to be widely used.

Position-dependent attenuation cannot be related to the possible existence of multiple scattering since all the measurements are carried out in the Rayleigh scattering region where multiple reflections are generally negligible. There is no clear explanation for the existence of position-dependent attenuation, and this cannot be related to the variation in grain size with position since the steel samples used are homogeneous. There are reports[24,25] which suggest that the rate of decay of the backscattered signal is initially dominated by scattering effects, but with depth, the effects of absorption become more dominant, which is less severe. Another possible cause of position-dependent attenuation can be related to the diffraction property of the ultrasonic beam. Nevertheless, from a practical point of view, the estimation of the attenuation coefficient must be confined to a known region in order to more meaningfully characterize the grain size based on the presence of decay in the backscattered signal.

The experiments for examining the position-dependent attenuation coefficient were based on spatial averaging since it performs slightly better than time averaging. In order to evaluate the position-dependent attenuation coefficient, the attenuation coefficient was estimated using a data window that corresponds to a 0.6 in. segment of the specimen. This window was applied to the traces shown in Fig. 8 and was shifted through the entire signal. The estimated attenuation coefficients via position of the window are shown in Fig. 12(a). In the beginning of the estimate, it is evident that the heat-treated steel sample with the smaller grain size (steel-1700) shows higher attenuation coefficient than the larger grain size sample (steel-2000). However, the attenuation of steel-1700 becomes less than the attenuation of steel-2000 at a later position. This inconsistent behavior in the estimation of the attenuation coefficients may be caused by inadequate data size, or by the high degree of variation in the characteristics of grain scattering. A consistent estimate can be obtained by using larger window size. For example, Fig. 12(b)

TABLE IV. Performance of temporal averaging.

| Window size (actual $N$) | 128 | 256 | 384 | 512 |
|---|---|---|---|---|
| Variance (0.1445) | 0.021 | 0.0032 | 0.0018 | 0.0011 |
| Effective $N$ | 6.8 | 45.2 | 77.9 | 134.5 |
| Normalized effective $N$ | 5% | 18% | 21% | 26% |

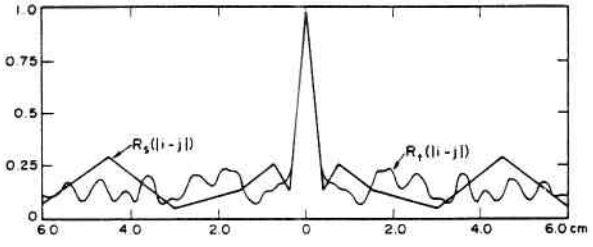


FIG. 11. Comparison of temporal and ensemble correlation functions.

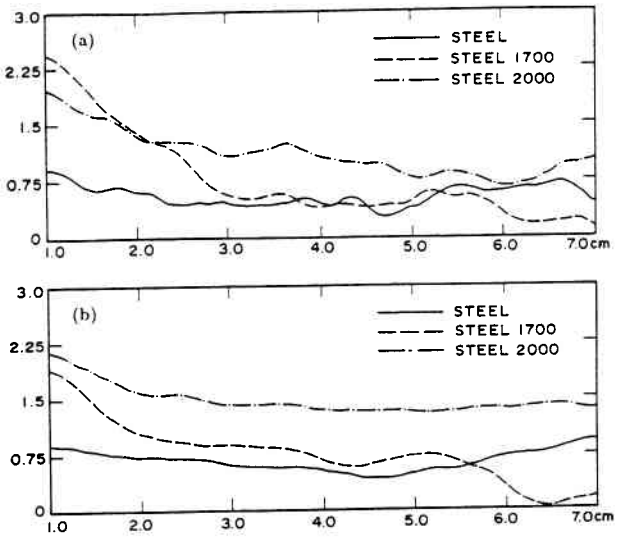


FIG. 12. Estimated position-dependent attenuation coefficient of the steel samples.

shows the results when using data window size corresponding to 1.2 in. of the sample. In this figure, the sample with the larger grain size shows higher attenuation compared to the sample with the smaller grain size. All three samples exhibit a change in the rate of attenuation as a function of position. Further inspection of this figure reveals that, although the estimation at the starting position shows higher attenuation for the larger grain sample, this may not be the case at a later position (i.e., deeper in the sample). This behavior can be influenced by the microstructure of the material, as well as the transducer beamwidth, center frequency, and bandwidth, and the size of the estimation window. Therefore, it is important that this technique be carefully evaluated prior to its utilization in routine nondestructive testing.

## V. CONCLUSION

It has been shown that it is feasible to characterize materials with different grain sizes by analyzing the backscattered signal. This has been achieved by measuring the attenuation coefficient using two equivalent approaches for smoothing the backscattered signal. Statistical analysis and experimental results suggest that the accuracy of the estimated attenuation coefficient using time averaging are very close to ensemble averaging. The choice of scanning steps for spatial averaging and the window length for temporal averaging are critical in the effectiveness of the smoothing operation. For all examined materials, the estimated attenuation coefficient was observed to be position dependent, such that its value decreases as the ultrasonic beam penetrates into the specimen. Therefore, the use of attenuation coefficient for grain size characterization must be confined to a fixed region of the specimen. Finally, it is important to point out that the smoothing procedure does not need to be carried out using ensemble or time averaging. In practice, a low-pass filter with a proper cutoff frequency is capable of generating similar results. Indeed, the proposed time averaging technique is a low-pass-filtering process which is simple to implement and provides information confined to a small region of the materials.

## ACKNOWLEDGMENTS

This project is supported by EPRI Grant RP2405-22.

[1]R. Klinman, G. R. Webster, F. J. Marsh, and E. T. Stephenson, "Ultrasonic Prediction of Grain Size, Strength, and Toughness in Plain Carbon Steel," Mater. Eval. **38** (10), 26–32 (1980).
[2]R. Klinman and E. T. Stephenson, "Ultrasonic Prediction of Grain Size and Mechanical Properties in Plain Carbon Steel," Mater. Eval. **39** (11), 1116–1120 (1981).
[3]J. W. Shilling, "Grain Boundary Demagnetizing Fields in 3% Si–Fe," J. Appl. Phys. **41**, 1165–1166 (1970).
[4]E. Adler and H. Pfeiffer, "The Influence of Grain Size and Impurities on the Magnetic Properties of the Soft Magnetic Alloy 47.5% NiFe," IEEE Trans. Magn. **10**, 172–174 (1974).
[5]K. Goebbels, "Structure Analysis by Scattered Ultrasonic Radiation," in *Research Techniques in Non-destructive Testing*, edited by R. Sharpe (Academic, New York, 1980).
[6]E. P. Papadakis, "Scattering in Polycrystalline Media," in *Method of Experimental Physics, Vol. 19, Ultrasonic*, edited by P. D. Edmonds (Academic, New York, 1981).
[7]D. Beecham, "Ultrasonic Scatter in Metals; Its Properties and Its Application to Grain Size Determination," Ultrasonics **4**, 67–76 (1966).
[8]E. E. Aldridge, "The Estimation of Grain Size in Metal," in *Non-destructive Testing*, edited by X. Egerton, Harwell Post-Graduate Series (Oxford U. P., Oxford, 1969), pp. 31–45.
[9]B. Fay, "Theoretical Consideration of Ultrasonic Backscattering," Acustica **28**, 354–357 (1973).
[10]V. Shimitz and K. Goebbels, "Improvement of Signal to Noise Ratio for the Ultrasonic Testing of Coarse Grained Materials by Digital RF-signal Averaging," IEEE Ultrason. Proc. 950–953 (1982).
[11]K. Goebbel, S. Hirsekorn, and H. Willems, "The Use of Ultrasound in the Determination of Microstructure," IEEE Ultrason. Proc., 841–846 (1984).
[12]J. Saniie and N. M. Bilgutay, "Quantitative Grain Size Evaluation Using Ultrasonic Backscattered Echoes," J. Acoust. Soc. Am. **80**, 1816–1824 (1986).
[13]E. P. Papadakis, "Ultrasonic Attenuation Caused by Scattering in Polycrystalline Metals," J. Acoust. Soc. Am. **37**, 703–710 (1965).
[14]W. P. Mason and H. I. McSkimin, "Attenuation and Scattering of High Frequency Sound Waves in Metals and Glasses," J. Acoust. Soc. Am. **19**, 464–473 (1947)
[15]A. Bhatia, "Scattering of High-Frequency Sound Waves in Polycrystalline Materials," J. Acoust. Soc. Am. **31**, 16–23 (1956).
[16]E. P. Papadakis, "Revised Grain Scattering Formulas and Tables," J. Acoust. Soc. Am. **37**, 711–717 (1965).
[17]E. P. Papadakis, "The Inverse Problem in Materials Characterization through Ultrasonic Attenuation and Velocity Measurements," in *Nondestructive Methods for Materials Properties Determination*, edited by D. Ruud and R. E. Green, Jr. (Plenum, New York, 1984), pp. 151–160.
[18]P. Beckmann, *Probability in Communication Engineering* (Harcourt, Brace and World, New York, 1967).
[19]J. Saniie, "Ultrasonic Signal Processing: System Identification and Parameter Estimation of Reverberant and Inhomogeneous Targets," Ph.D. thesis, Purdue University, Lafayette, IN, 1981.
[20]F. E. Nathanson, *Radar Design Principles* (McGraw-Hill, New York, 1969).
[21]D. K. Barton, Editor, "Radar Clutter," in *Radars* (Artech House, Dedham, MA, 1977), Vol. 5.
[22]J. Saniie, N. M. Bilgutay, and D. T. Nagle, "Evaluation of Signal Processing Schemes in Ultrasonic Grain Size Estimation," in *Review of Progress in Quantitative Nondestructive Evaluation, 5A*, edited by D. O. Thompson and D. E. Chimenti (Plenum, New York, 1986), pp. 747–753.
[23]R. G. Gallager, *Information Theory and Reliable Communication* (Wiley, New York, 1968), Chap. 2.
[24]H. Willems, "A New Methods for the Measurement of Ultrasonic Absorption in Polycrystalline Materials," in *Review of Progress in Quantitative Nondestructive Evaluation, 6A*, edited by D. O. Thompson and D. E. Chimenti (Plenum, New York, 1987), pp. 473–481.
[25]J. F. Bussiere, "Application of NDE to the Processing of Metal," in *Review of Progress in Quantitative Nondestructive Evaluation, 6B*, edited by D. O. Thompson and D. E. Chimenti (Plenum, New York, 1987), pp. 1377–1393.